OXFORD

JNCI J Natl Cancer Inst (2017) 109(3): djw236

doi: 10.1093/jnci/djw236
First published online February 10, 2017
Article

ARTICLE

Estrogen Receptor β as a Therapeutic Target in Breast Cancer Stem Cells

Ran Ma, Govindasamy-Muralidharan Karthik, John Lövrot, Felix Haglund, Gustaf Rosin, Anne Katchy, Xiaonan Zhang, Lisa Viberg, Jan Frisell, Cecilia Williams, Stig Linder, Irma Fredriksson, Johan Hartman

Affiliations of authors: Department of Oncology and Pathology (RM, GMK, JL, FH, XZ, LV, SL, JH), Cancer Center Karolinska (RM, GMK, JL, FH, GR, XZ, LV, SL, JH), and Department of Molecular Medicine and Surgery (JF, IF), Karolinska Institutet, Stockholm, Sweden; Department of Biosciences and Nutrition, Karolinska Institutet, Huddinge, Sweden (GR, CW); Center for Nuclear Receptors and Cell Signaling, Department of Biology and Biochemistry, University of Houston, Houston, TX (AK, CW); Department of Pathology and Cytology, Karolinska University Laboratory, Stockholm, Sweden (FH, JH); Department of Breast and Endocrine Surgery, Karolinska University Hospital, Stockholm, Sweden (JF, IF); Science for Life Laboratory, Department of Proteomics, KTH, Royal Institute of Technology, Stockholm, Sweden (CW); Department of Medical and Health Sciences, Department of Medicine and Health, Linköping University, Linköping, Sweden (SL);

Correspondence to: Johan Hartman, M.D., PhD, Department of Oncology and Pathology, Karolinska Institutet, 17176 Stockholm, Sweden (e-mail: johan.hartman@ki.se).

Abstract

Abstract Background: Breast cancer cells with tumor-initiating capabilities (BSCs) are considered to maintain tumor growth and govern metastasis. Hence, targeting BSCs will be crucial to achieve successful treatment of breast cancer.
Methods: We characterized mammospheres derived from more than 40 cancer patients and two breast cancer cell lines for the expression of estrogen receptors (ERs) and stem cell markers. Mammosphere formation and proliferation assays were performed on cells from 19 cancer patients and five healthy individuals after incubation with ER-subtype selective ligands. Transcriptional analysis was performed to identify pathways activated in ERβ-stimulated mammospheres and verified using in vitro experiments. Xenograft models (n = 4 or 5 per group) were used to study the role of ERs during tumorigenesis.
Results: We identified an absence of ERα but upregulation of ERβ in BSCs associated with phenotypic stem cell markers and responsible for the proliferative role of estrogens. Knockdown of ERβ caused a reduction of mammosphere formation in cell lines and in patient-derived cancer cells (40.7%, 26.8%, and 39.1%, respectively). Gene set enrichment analysis identified glycolysis-related pathways (false discovery rate < 0.001) upregulated in ERβ-activated mammospheres. We observed that tamoxifen or fulvestrant alone was insufficient to block proliferation of patient-derived BSCs while this could be accomplished by a selective inhibitor of ERβ (PHTPP; 53.7% in luminal and 45.5% in triple-negative breast cancers). Furthermore, PHTPP reduced tumor initiation in two patient-derived xenografts (75.9% and 59.1% reduction in tumor volume, respectively) and potentiated tamoxifen-mediated inhibition of tumor growth in MCF7 xenografts.
Conclusion: We identify ERβ as a mediator of estrogen action in BSCs and a novel target for endocrine therapy.

The existence of breast cancer cells with stem cell–like capacity has been suggested as a likely explanation to therapeutic resistance and tumor relapse (1). Serial passaging of cells growing as nonadherent spheres can be applied to isolate and propagate both normal mammary stem cells (MSCs) and breast cancer stem cells (BSCs) (1,2). BSCs are highly tumorigenic in mouse transplantation assays compared with differentiated cancer cells (3). In addition, the majority of mammospheres are phenotypically CD24(-), CD44(+), EpCAM(+) (3,4), and/or with high activity of aldehyde dehydrogenase 1 (ALDH1) (5,6).

Approximately 75% of all breast cancers are positive for estrogen receptor (ER)α (ESR1), which in turn positively correlates with response to endocrine therapy (7). The second estrogen receptor, ERβ (ESR2), has in some studies been associated with improved survival in tamoxifen-treated patients (8–10). The two ER subtypes are encoded by genes on different chromosomes

Received: October 16, 2014; **Revised:** August 15, 2016; **Accepted:** September 20, 2016

and activate estrogen response elements (ERE) in reporter gene assays (11). Although considered ERα-negative, BSC and MSC numbers can be expanded by incubation with estradiol (12,13), previously explained by paracrine stimulation (14,15). To dissect the role of estrogen receptors within BSCs, we performed a comprehensive analysis of mammospheres generated from patient-derived cancer cells and from normal benign breast epithelium.

Methods

Clinical Material

Between 2009 and 2015, fresh primary breast cancer specimens from 88 patients were collected at the Karolinska University Hospital. Biobanking was approved by the local biobank board and the Department of Pathology. Experimental procedures and protocols were approved by the regional ethics review board (Etikprövningsnämnden) in Stockholm. Tumor tissues with corresponding clinical data were obtained after signed informed consent from each patient. Anonymized normal breast specimens from elective reduction mammoplasties at the Capio St Göran's Hospital, Stockholm, Sweden, were also used.

Mouse Experiments

All mouse experiments were approved by the local animal welfare board at Karolinska Institutet and in accordance with institution guidelines. Intact or ovariectomized SCID/NOD female mice three to eight weeks old were transplanted with MCF7 cells, MDA-MB-231 cells, or patient-derived breast tumor fragments HCI001 and HCI002 into the fourth mammary gland fat pad. Four or five mice per group were assigned to different treatment conditions according to the aims of each experiment. Exact numbers are given in the "Results" and in the figure legends. Detailed procedures are provided in the Supplementary Materials (available online).

Statistical Analyses

Two-tailed *t* test was used to test statistical significance in the assays, real-time quantitative polymerase chain reaction (qPCR) experiments, and mouse experiments. Tests were either paired or independent depending on experimental setup (paired or unpaired samples). Extreme outlier values of technical causes (<10% of samples per group) have been excluded from analysis. Kruskal-Wallis nonparametric test was used to compare the ERβ protein expression between the molecular subtypes. Spearman's rank order correlation was used to test the association between ERβ and ERα expression. A Pvalue equal to or less than .05 was considered statistically significant.

For detailed information on all other experimental methods, please see the Supplementary Materials (available online).

Results

Expression of ERβ in Normal and Malignant Mammary Stem Cells

ERβ protein expression in tumors was analyzed by immunohistochemistry in a cohort of 187 patients with available gene expression–based subclass categorization (16). In contrast to ERα expression, concentrated within the luminal subtypes, the mean grading of ERβ staining ($P < .49$) was not associated with any certain molecular subtype, and no correlation was found between the ERα mRNA and ERβ protein expression profiles as assessed by Spearman rank correlation ($P = .98$, $\rho = .0017$) (Figure 1A; Supplementary Figure 1A, available online). Next, dual immunohistochemical staining with ERβ and CD44 was performed, showing ERβ protein expression in 79.2% of all breast tumors. In 71.0% of the tumors, ERβ was detected within the CD44(+) cell population (Figure 1B).

We further confirmed that patient-derived mammospheres were ERα(–) as described before (17), but we also observed a strong ERβ nuclear positivity (>80.0% of mammospheres) (Figure 1C). Interestingly, BSCs from triple-negative breast cancers (ERα[-]/PR[-]/Her2[-]), clinically considered estrogen independent, stained positive for ERβ with similar intensity (three patients). We were able to prove that mammospheres were enriched for BSCs as the vast majority of mammospheres were CD44(+)/CD24(-), $ALDH1^{High}$ (>95.0%), and positive for PKH26 (Figure 1C), a marker for quiescence (18). ERβ was also co-expressed with CD44 or ALDH1 in 26 out of 26 tumors, as well as in the majority of EpCAM (4) and PKH26-positive mammospheres. To explore the potential role of ERβ in MSCs, we analyzed ERβ expression in mammopsheres from patients undergoing reduction mammoplasties. Similar to BSCs, MSCs (n = 16 patients) were all ERα-negative and mostly ERβ-positive and co-expressed CD44 and ALDH1 (Supplementary Figure 1, B–D, available online). Again, we confirmed the similarity of MCF7 (luminal-like) and MDA-MB-231 (basal-like) spheres to patient-derived mammospheres (Figure 1, D and E). *ERβ* and the embryonic pluripotency genes *SOX2*, *NANOG*, and *OCT4* (20) were induced five to 11 times in nonadherent mammospheres compared with the adherent counterparts (Supplementary Figure 1, E and F, available online), and this coincided with a switch from $ERα^{High}/ERβ^{Low}$ to $ERα^{Low}/ERβ^{High}$ during mammosphere formation (Figure 1, D and E). Together, our observations reveal that ERβ is the predominant estrogen receptor in MSCs as well as in BSCs.

Impact of Altered ERβ Expression on the Cancer Stem Cell Phenotype

To assess the importance of ERβ for maintenance of the BSC state, we produced MCF7 cells with shRNA-mediated knockdown of ERβ (Supplementary Figure 2, A–C, available online), resulting in 40.7% reduction ($P < .01$) of mammosphere formation (Figure 2A). A similar effect was seen in MDA-MB-231 cells (26.8% reduction, $P < .04$) (Supplementary Figure 2E, available online). Importantly, cells without ERβ overexpression could not maintain mammosphere formation after the sixth generation, whereas cells with ERβ overexpression maintained their increased mammosphere-forming capacity throughout the experiment (Figure 2B). By forced differentiation of patient-derived BSCs in normal serum-containing medium, we observed a 70.0% and 60.0% reduction of cellular ERβ and ALDH1 expression, respectively (Figure 2C), underscoring a tight connection between ERβ expression and the stem cell state. To confirm our findings, ERβ was knocked-down by lentiviral-mediated shRNA in patient-derived BSCs. Nuclear ERβ expression was silenced in 60.0% to 85.0% of the mammosphere cells, and, as expected, ERβ silencing in BSCs caused a profound decrease in total number of mammospheres (39.1% reduction, $P = .03$) (Figure 2D). We observed that cells with silenced ERβ also lost the expression of ALDH1 whereas CD44-intensity was unchanged, giving further support to the importance of ERβ to maintain the BSC state (Figure 2E; Supplementary Figure 2D, available online).

ARTICLE

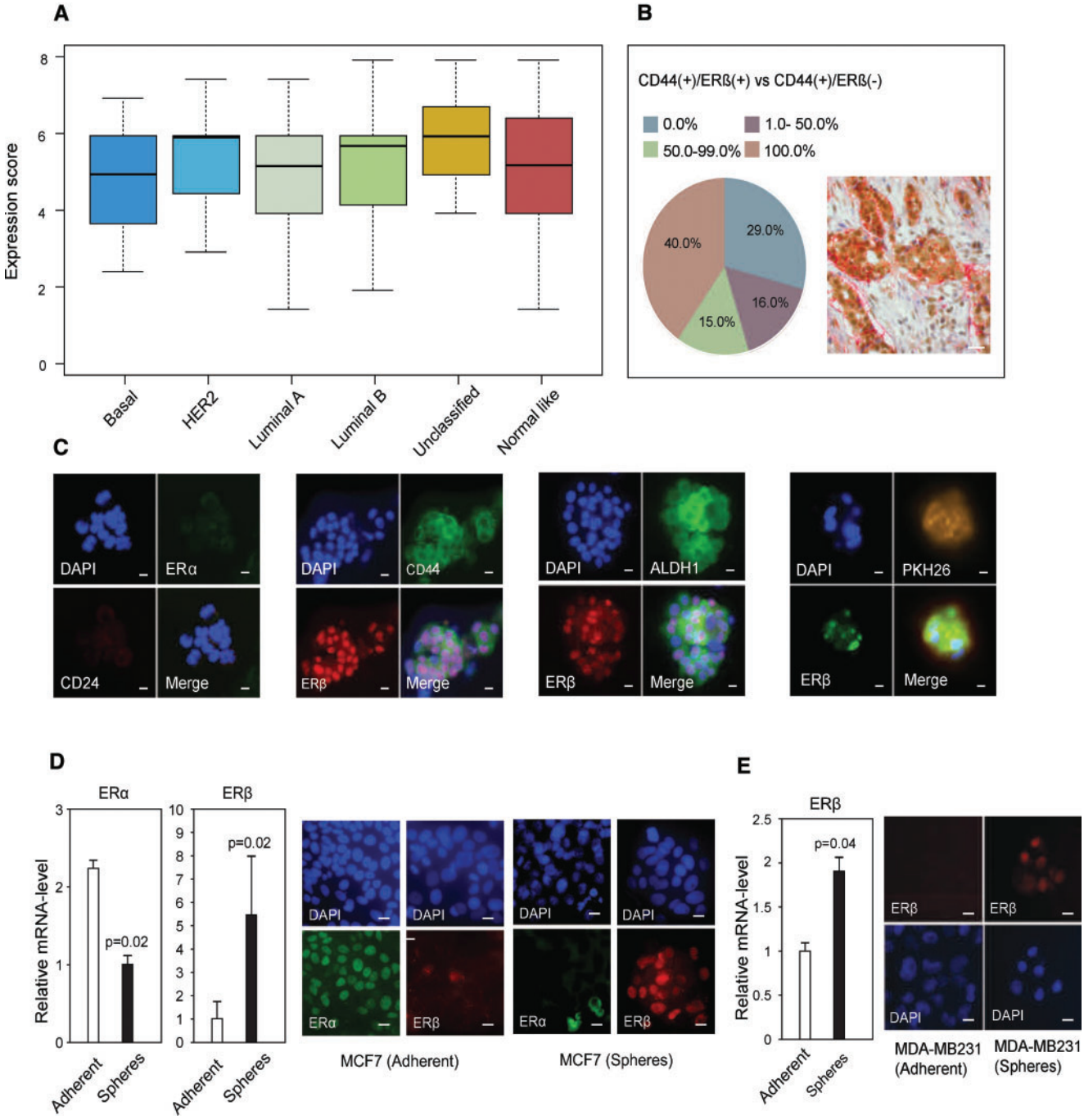

Figure 1. Evaluation of estrogen receptor (ER)β levels in breast cancer stem cells. **A)** Correlation between ERβ protein expression (PPG5/10) and molecular subclass category analyzed in 187 patients. The mean grading of ERβ was not statistically significantly different between subtypes (Kruskal-Wallis, $P < .49$). Mean expression scores are presented. **Error bars** represent SD. **B)** Relative number of CD44-positive (CD44+) cells that also express ERβ in breast cancer tumors, based upon immunohistochemistry. In 40.0% of the tumors, 100.0% of the CD44+ cells were also positive for ERβ (**red**). In 15.0% of the tumors, 50.0%–99.0% of the CD44+ cells also expressed ERβ (**green**). In 16.0% of the tumors, 1.0%–50.0% of the CD44+ cells also expressed ERβ (**purple**), whereas 29.0% of the tumors did not express any ERβ in the CD44+ cells (**blue**). In total, 71.0% of the patients showed ERβ/CD44 co-expression. Representative dual immunohistochemistry image is shown in **the right corner** (ERβ: **brown**, CD44: **red**). **Scale bar** = 100 μm. **C)** Dual immunofluorescence imaging of patient-derived breast cancer cells with tumor-initiating capabilities in the following order: ERα (**green**) and CD24 (**red**), ERβ (**red**) and CD44 (**green**), ERβ (**red**) and ALDH1 (**green**), ERβ (**green**) and PKH26-staining (**yellow/brown**). All counterstaining with DAPI (**blue**). **Scale bar** = 10 μm. **D) Left panel**: quantitative polymerase chain reaction (qPCR) analysis of ERα and ERβ (Student's *t* test, mean ± SD, 3 replicates) in MCF7-adherent cells (**white bars**) and spheres (**black bars**). **Right panel**: Immunofluorescence imaging of MCF7 adherent cells and spheres: ERα (**green**) and ERβ (**red**) counterstained with DAPI (**blue**). **Scale bar** = 10 μm. **E) Left panel**: qPCR analysis of ERβ (Student's *t* test, mean ± SD, 3 replicates) in MDA-MB-231-adherent cells and MDA-MB-231-derived spheres. **Right panel**: Immunofluorescence imaging of MDA-MB-231-adherent cells and MDA-MB-231 spheres: ERβ (**red**) counterstained with DAPI (**blue**). **Scale bar** = 10 μm. All statistical tests were two-sided. DAPI = 4',6-diamidino-2-phenylindole; ER = estrogen receptor; HER2 = human epidermal growth factor receptor.

ARTICLE

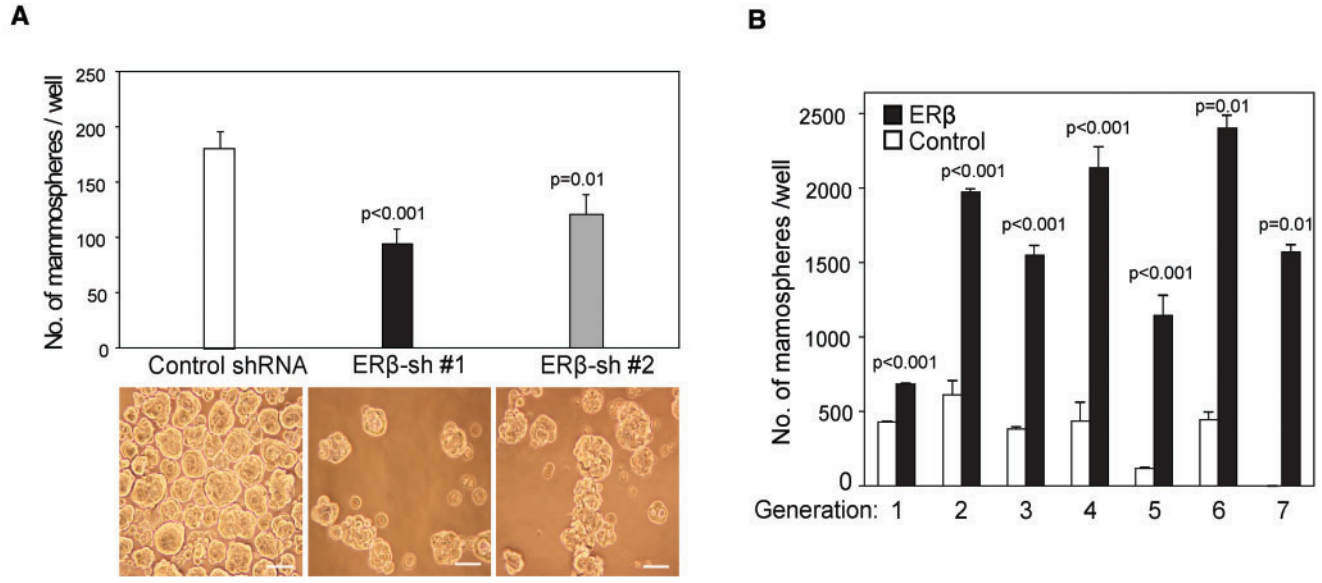

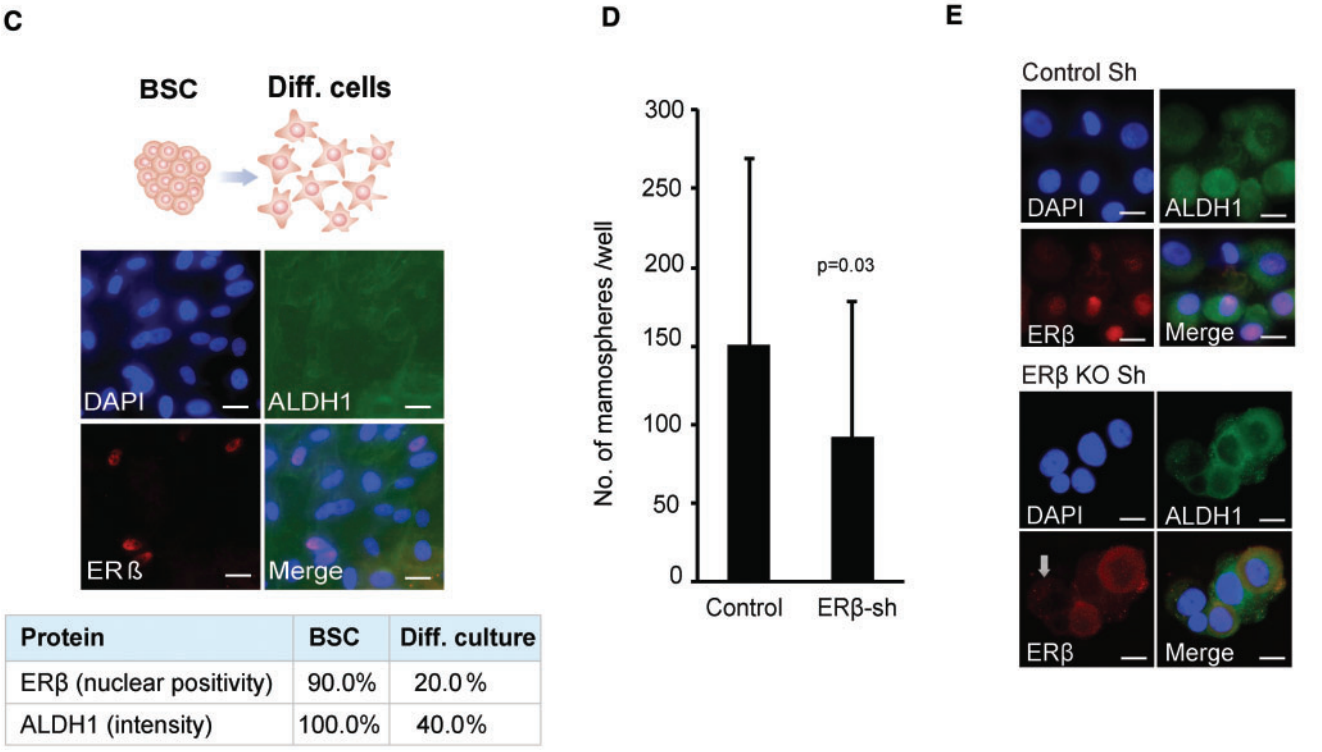

Protein	BSC	Diff. culture
ERβ (nuclear positivity)	90.0%	20.0%
ALDH1 (intensity)	100.0%	40.0%

Figure 2. Estrogen receptor (ER)β and the cancer stem cell phenotype. **A)** Average number of mammospheres in control vs shRNA-ERβ knockdown clones generated from 2000 MCF7 cells after seven days of incubation in nonadherent conditions, with representative images presented below each bar (Student's *t* test, mean ± SD, 3 replicates). **Scale bar** = 100 μm. **B)** Number of mammospheres formed by MCF7 cells, with transduced ERβ expression (**black bar**) and without (**white bar**) over seven passages. An equal number of cells was seeded for each passage (Student's *t* test, mean ± SD, 3 replicates). **C)** Forced differentiation of breast cancer cells with tumor-initiating capabilities by incubation in selective medium supplemented with 5% fetal bovine serum induced a switch from nonadherent to a spindle-like, adherent cell phenotype and stained for ERβ and ALDH1 (n = 8 patients). **Scale bar** = 10 μm. **D)** Numbers of patient-derived mammospheres after lentiviral shRNA-mediated knockdown of ERβ compared with treatment with the nontargeted scrambled shRNA construct as control. Following lentiviral transduction, cells were incubated in selective medium for seven days (Student's *t* test, mean ± SD, n = 4 patients, 4 replicates). **E)** Immunofluorescence imaging of patient-derived cells after lentiviral shRNA-mediated knockdown of ERβ, with antibodies for ERβ (**red**) and ALDH1 (**green**) counterstained with DAPI (**blue**). **Scale bar** = 10 μm. All statistical tests were two-sided. ALDH1 = Aldehyde dehydrogenase 1; BSC = breast cancer cells with tumor-initiating capabilities; DAPI = 4',6-diamidino-2-phenylindole; ER = estrogen receptor; sh = small hairpin RNA.

ARTICLE

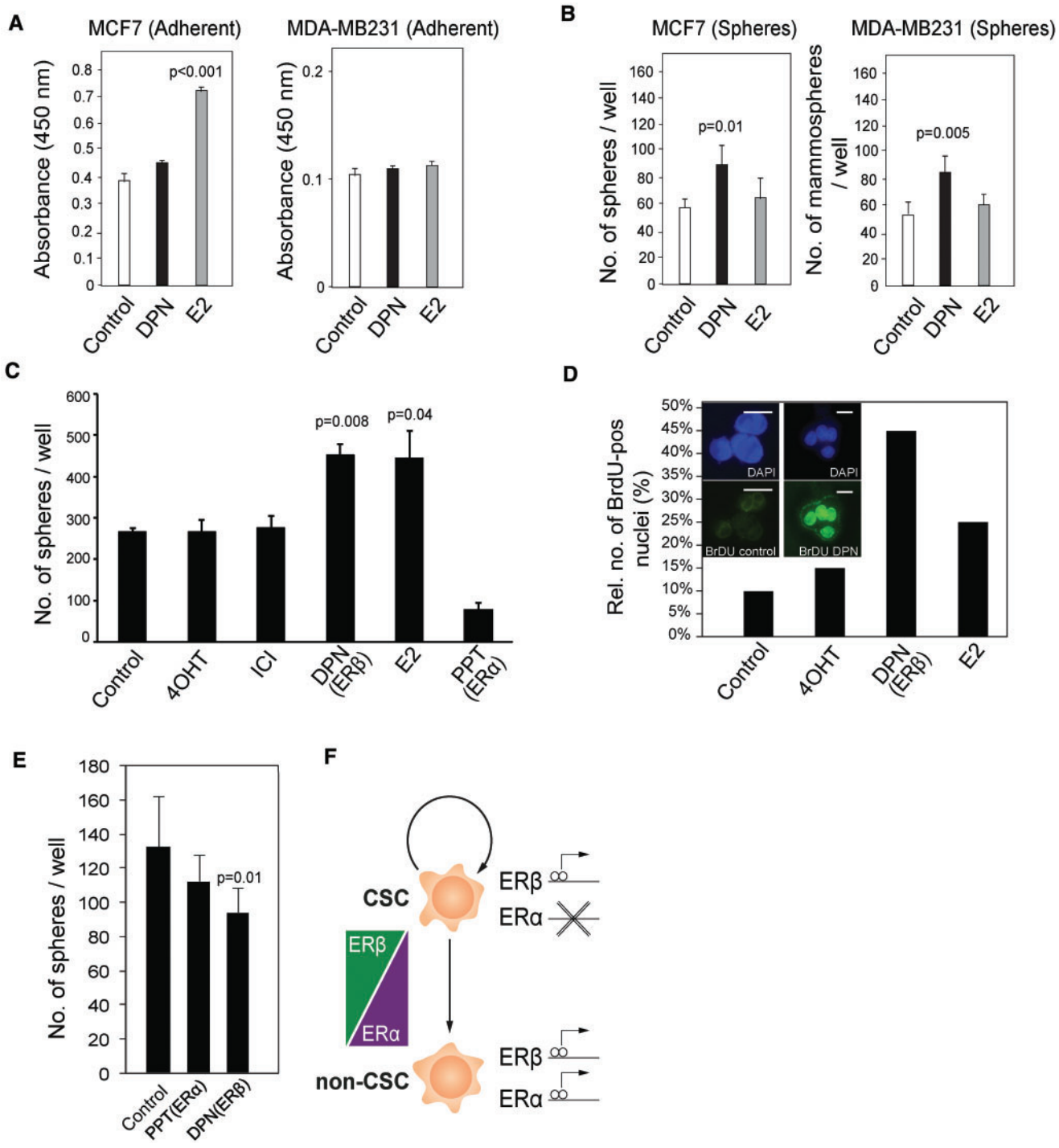

Figure 3. Regulation of breast cancer cells with tumor-initiating capabilities, proliferation by selective estrogen receptor modulators. **A)** WST-1 assay was performed on MCF7- and MDA-MB-231-adherent cells (5000 cells, Student's *t* test, mean ± SD, 3 replicates) during four days of treatment with estradiol (E2) and diarylproprionitrile (DPN) at 10 nM concentration. **B)** Mammosphere formation assay was carried out using MCF7 and MDA-MB-231 cells (2000 cells, Student's *t* test, mean ± SD, 3 replicates) during seven days with E2 and DPN treatment at 10 nM concentration. Mammospheres were manually counted using a brightfield microscope. **C)** Mammosphere formation from patient-derived cancer cells; 500–1000 cells from dissociated primary breast cancer mammospheres were seeded and incubated together with 10 nM E2, 100 nM 4-hydroxytamoxifen (4OHT), 10 nM ICI-182,780 (fulvestrant), 10 nM DPN, 10 nM propylpyrazoletrisphenol (PPT), or vehicle control for 12 days. (Student's *t* test, mean ± SD, n = 12 patients, 4 replicates). **D)** Single cells from dissociated primary mammospheres treated as described above were incubated with 10 μM BrdU in conditional medium for 72 hours. Absolute number of BrdU-positive cells was estimated under fluorescent microscope. Representative immunofluorescent staining and bar plot representing the relative percentage of positive BrdU cells from one patient. **Scale bar** = 10 μm. **E)** Formation of mammospheres from mammary stem cells (MSCs); 4–5000 primary mammary epithelial cells plated onto 48-well plates and incubated with 10 nM DPN, 10 nM PPT, and vehicle control for 12 days (Student's *t* test, mean ± SD, n = 5 patients, 4 replicates). **F)** Hypothetical model of estrogen receptor (ER)α and ERβ action in CSCs vs differentiated cancer cells. All statistical tests were two-sided. 4OHT = 4-hydroxytamoxifen; CSC = cancer stem cells; DPN = diarylproprionitrile; ER = estrogen receptor; PPT = propylpyrazoletrisphenol. ICI-182,780 = 7α,17β-[9-[(4,4,5,5,5-Pentafluoropentyl)sulfinyl]nonyl]estra-1,3,5(10)-triene-3,17-diol.

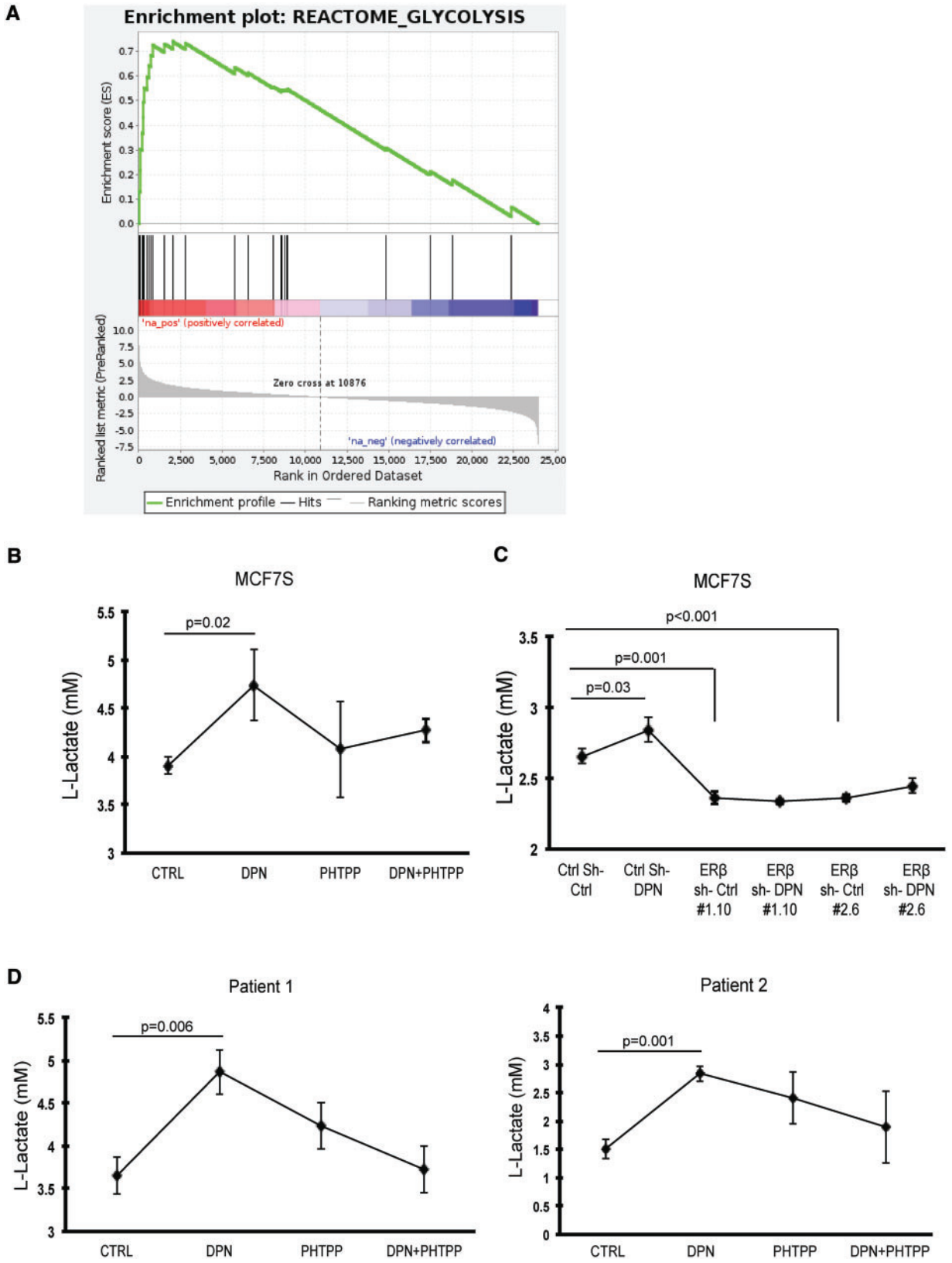

Figure 4. Glycolytic metabolism regulated by estrogen receptor (ER)β. **A)** Gene set enrichment plot of statistically significantly upregulated pathways in diarylproprionitrile (DPN) stimulated MCF7S (false discovery rate < 0.001). **B)** MCF7 spheres were seeded into selective medium as single cells at 10 000 cells/well in the presence of 10 nM DPN, 100 nM PHTPP, combined treatment, and vehicle control. After 24-hour incubation, secreted L-lactate concentrations in the culture supernatants were determined (Student's *t* test, mean ± SD, 5 replicates). **C)** MCF7 scramble shRNA cells and ERβ knockdown clones were seeded into selective medium at 10 000 cells/well, supplied with 10 nM DPN over 24 hours. Secreted L-lactate concentrations in the culture supernatants were determined (Student's *t* test, mean ± SD, 5 replicates) afterward. **D)** Stable spheres from two patients were seeded as single cells into selective medium at 5000 cells/well. Treatments were given as 10 nM DPN, 100 nM PHTPP, combined treatment, and vehicle control. Secreted L-lactate concentrations in the culture supernatants were determined (Student's *t* test, mean ± SD, n = 2 patients, 5 replicates) after 24 hours of incubation.

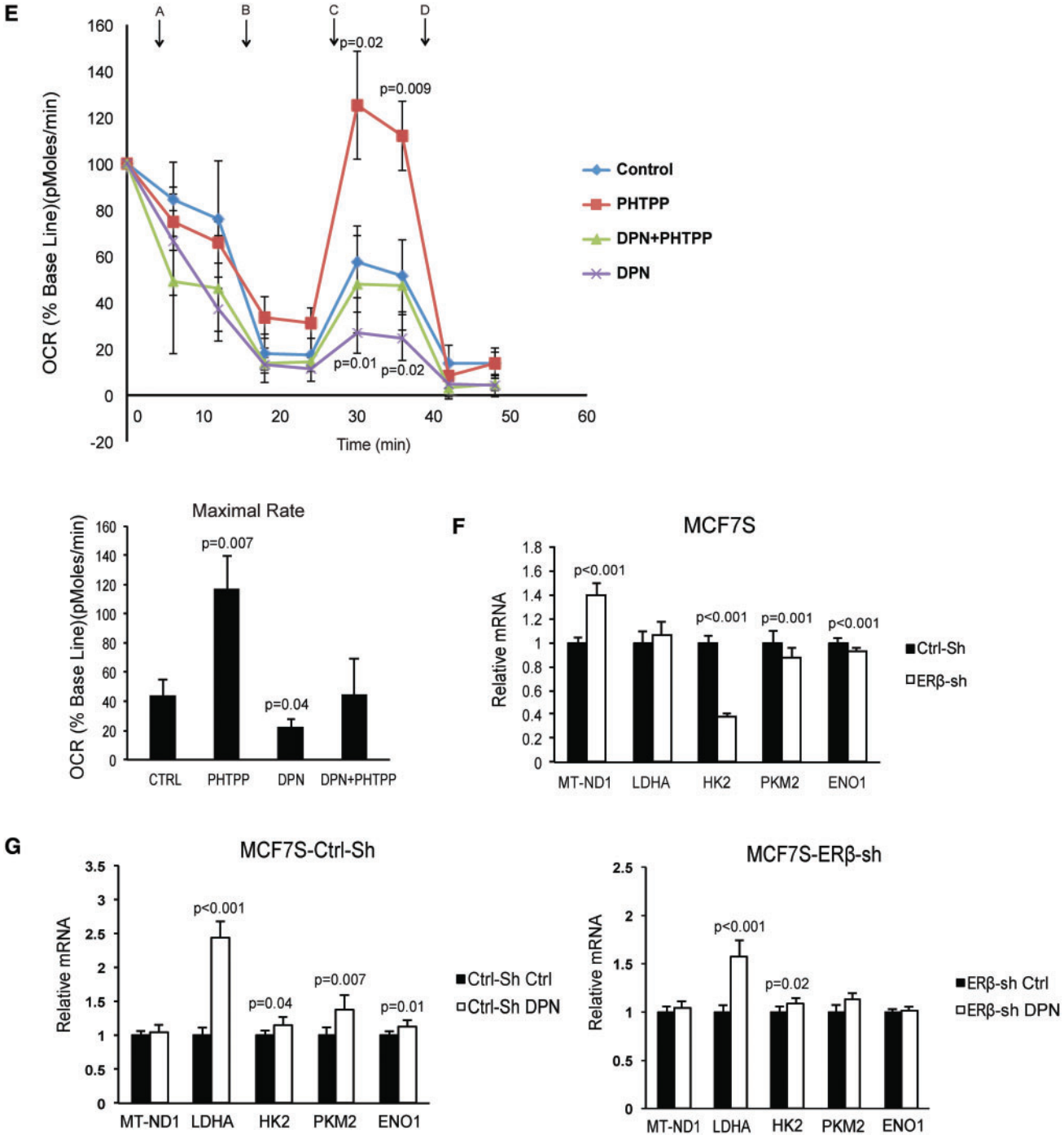

Figure 4. (continued) **E) Upper panel**: Time course of oxygen consumption rate (OCR) changes were measured during different incubations: 10 nM DPN, 100 nM PHTPP, combined treatment, and vehicle control in first-generation MCF7 spheres. Statistical significance was calculated between PHTPP or DPN vs control group, respectively (Student's *t* test, mean ± SD, 4 replicates). **Arrows** represent the following reagents used during the time course of measurements. A: glucose; B: oligomycin-ATP coupler; C: FCCP (carbonyl cyanide p-trifluoromethoxyphenylhydrazone)–electron transport chain accelerator; D: rotenone+antimycin–mitochondria inhibitors. **Lower panel**: Quantification of maximal rate (FCCP OCR–rotenone+antimypcin OCR) (Student's *t* test, mean ± SD, 4 replicates). **F)** Relative mRNA expression levels of mitochondrial *ND-1* and glycolytic enzymes in first-generation spheres from ERβ knockdown MCF7 as compared with scrambled vehicle control MCF7 (Student's *t* test, mean ± SD, 6 replicates). **G) Left panel**: relative mRNA expression levels of mitochondrial *ND-1* and glycolytic enzymes in first-generation spheres from scrambled control shRNA MCF7 treated with DPN as compared with scrambled vehicle control (Student's *t* test, mean ± SD, 6 replicates). **Right panel**: The relative mRNA expression levels of the same genes in first-generation spheres from ERβ knockdown MCF7 treated with DPN as compared with vehicle control (Student's *t* test, mean ± SD, 6 replicates). All statistical tests were two-sided. DPN = diarylproprionitrile; ENO1 = enolase 1; ER = estrogen receptor; HK2 = hexokinase 2-HK2; LDHA = lactate dehydrogenase A; MT-ND1 = mitochondrial NADH:ubiquinone oxidoreductase core subunit 1; NES = normalized enrichment score; PKM2 = pyruvate kinase muscle 2; sh = small hairpin RNA.

Proliferative Role of ERβ in BSCs, MSCs, and Differentiated Cancer Cells

Although 17β-estradiol (E2) induces proliferation of adherent MCF7 cells, the ERβ-selective agonist diarylproprionitrile (DPN) did not affect proliferation of adherent MCF7 or MDA-MB-231 cells (Figure 3A). However, incubation with DPN increased the number of mammospheres from both cell lines compared with the vehicle controls ($P = .01$ and $P = .005$, respectively) (Figure 3B). This finding was also confirmed with patient-derived primary tumor cells, where incubation with DPN and E2 increased mammosphere numbers by 70.6% ($P = .008$) and 67.7% ($P = .04$), respectively (Figure 3C). This effect was corroborated by BrdU staining after similar incubations (Figure 3D). However, the ERα-selective agonist propylpyrazoletrisphenol (PPT) did not affect the number of mammospheres, nor did 4-hydroxytamoxifen (4OHT) or fulvestrant (Figure 3C). When the same treatments were applied to MSCs, stimulation of ERβ by DPN caused a dramatic reduction (29.1%, $P = .01$) in mammosphere formation, indicating that ERβ is not proliferative in the MSC population (Figure 3E).

In addition, treatment of MCF7 spheres with DPN increased embryonic stem cell gene expression, as well as of the ER-target genes *PR* and *PS2* (23,24). In adherent cells, however, DPN treatment did not affect those genes, although PR was induced (Supplementary Figure 3, available online). As a consequence of our findings, we hypothesize that a switch in ER dependence of cancer cells occurs in the adherent (differentiated) vs mammosphere (stem-like) state (Figure 3F).

Functional Role of ERβ in Breast Cancer Stem Cells

To further explore ERβ function in BSCs, we performed whole-transcriptome analysis of mammospheres (MCF7S) incubated with vehicle control or DPN. Seventy-five transcripts were differentially regulated upon DPN treatment compared with the control group (moderated *t* tests, nominal $P < .001$, false discovery rate [FDR] ≈ 0.15) (Supplementary Table 2, available online). To assess the biological relevance of the distinct gene expression pattern, we performed gene set enrichment analyses (GSEA) of the canonical pathways gene set collection in the Molecular Signatures Database (Broad Institute). Seven gene sets were statistically significantly enriched in DPN-treated mammospheres compared with the control (FDR < 0.10) (Supplementary Table 2, available online), with the majority related to glycolytic metabolism and with REACTOME_GLYCOLYSIS as top pathway (FDR < 0.001) (Figure 4A).

Furthermore, we detected the L-lactate releasing amount in MCF7S culture medium as an indicator of cellular glycolytic rate. We used the ERβ-selective antagonist 4-[2-Phenyl-5,7*bis* (trifluoromethyl) pyrazolo[1,5-*a*]pyrimidin-3-yl]phenol (PHTPP) to validate the specificity of DPN and to inhibit ERβ function (25). After incubation with DPN, L-lactate secretion increased statistically significantly (23.1% induction, $P = .02$) compared with the control group, and this induction could be neutralized by cotreatment with PHTPP (Figure 4B). To confirm an ERβ-mediated effect, we employed ERβ-knockdown of MCF7 cells and performed the identical assay. The stimulation of the glycolytic shift could only be observed in the scrambled control supplied with DPN, but was absent in two knockdown clones after similar treatments (Figure 4C). To test the hypothesis on the clinical level, we generated patient-derived BSCs and observed increased L-lactate secretion in response to DPN from both patients (36.1% induction, $P = .006$, and 86.7% induction, $P = .001$) (Figure 4D). We also measured the oxygen consumption rate (OCR) after incubation with selective ER ligands. As expected, DPN stimulation in MCF7S undermined OCR. Accordingly, this metabolic phenotype can be overturned by PHTPP (Figure 4E, upper panel). We further determined the mitochondrial function by evaluation of maximal respiration rates. Consequently, PHTPP treatment resulted in a favorable 2.7-fold elevation ($P = .007$) of maximal respiratory capacity, while DPN treatment caused a two-fold decrease ($P = .04$) compared with the control (Figure 4E, lower panel). Hence, suppressing ERβ induces a substantial capacity for oxidative metabolism. Although the strongest OCR shift was observed in the first-generation mammospheres, there was a statistically nonsignificant but consistent trend of OCR changes retained in the third-generation mammospheres (Supplementary Figure 4A, available online). Together, our data suggest that the maintenance of the BSC phenotype relies on ERβ-mediated shifting of glycolysis. We also investigated the expression levels of glycolysis key enzymes and the mitochondrial respiration complex in scrambled control MCF7S and ERβ-knockdown MCF7S. We observed a 40.0% induction ($P < .001$) of mitochondrial NADH:ubiquinone oxidoreductase core subunit 1 (MT-ND-1) in ERβ knockdown-MCF7S and reduction of the majority of glycolytic enzymes (hexokinase 2-HK2, pyruvate kinase muscle 2–PKM2, and enolase 1-ENO1), although lactate dehydrogenase A (LDHA) mRNA was unchanged (Figure 4F). Again, when the comparisons were made within the scrambled control and ERβ knockdown clone, respectively, the variations of all genes induced by DPN were higher when ERβ was present (Figure 4G). Confocal microscopy after immunofluorencence staining of MCF7S wild-type and ERβ-knockdown MCF7 implied that DPN stimulation of presented ERβ could impair the quantity of mitochondria in the cells (Supplementary Figure 4, B and C, available online). Together, our results suggest that stimulating ERβ brings the BSCs pool toward glycolysis, partially because of the suppression of mitochondrial respiration and attenuation of mitochondrial biogenesis.

ERβ and Breast Tumor Growth in Mouse Xenografts

To assess ERβ's role in tumorigenesis, we transplanted adherent MCF7 cells into the mammary fat pad of ovariectomized NOD/SCID-mice. In absence of ER ligands, tumors remained very small whereas daily injections with DPN caused a three-fold increase ($P = .03$) in tumor volume after five weeks without any increase in uterus weight, commonly considered as an indicator of ERα activation. PPT treatment caused a six-fold increase ($P = .02$) in tumor volume, most probably reflecting the low ERβ/ERα ratio in differentiated MCF7 cells. However, the combination of PPT and DPN resulted in the largest tumor volumes ($P = .01$) (Figure 5A; Supplementary Figure 5A, available online). We thereby conclude that both ER subtypes are important for tumor growth.

Next, we injected MCF7-derived mammospheres into the mammary fat pads of ovariectomized NOD/SCID mice. Treatment with E2 resulted in the largest tumors, reflecting the activation of both ERα and ERβ during tumor progression (Supplementary Figure 5C, available online). DPN caused a six-fold induction ($P = .02$) in tumor volume compared with the untreated control. Importantly, the E2-induced tumor volume was reduced by 43.3% ($P = .04$) by cotreatment with PHTPP (Figure 5B; Supplementary Figure 5B, available online).

Again, to study the importance of ERβ during tumor initiation within the triple-negative phenotype, we transplanted

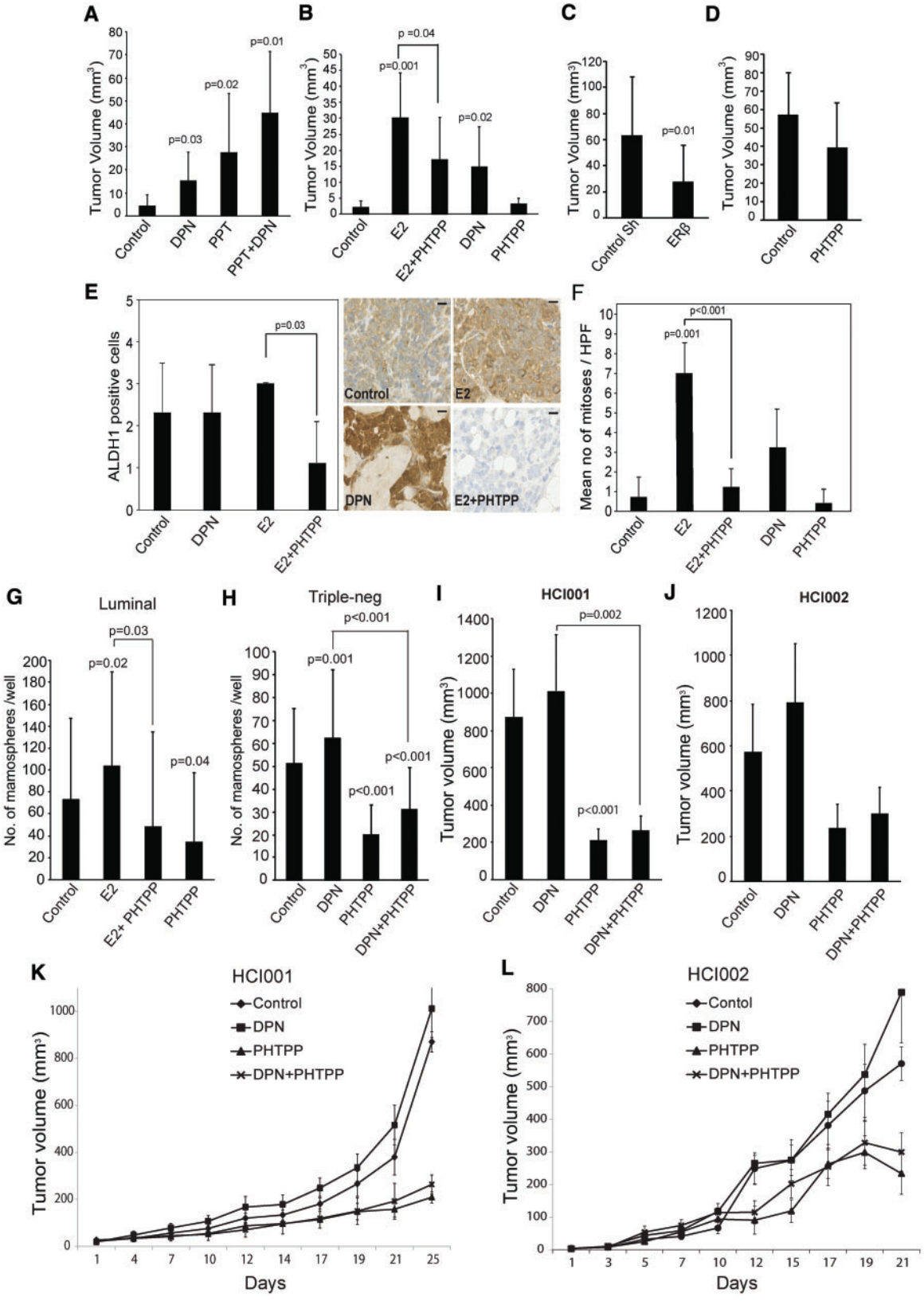
A
Tumor Volume (mm3)
p=0.03
p=0.02
p=0.01
Control
DPN
PPT
PPT+DPN
B
Tumor Volume (mm3)
p =0.04
p=0.001
p=0.02
Control
E2
E2+PHTPP
DPN
PHTPP
C
Tumor Volume (mm3)
p=0.01
Control Sh
ERβ
D
Tumor Volume (mm3)
Control
PHTPP
E
ALDH1 positive cells
p=0.03
Control
DPN
E2
E2+PHTPP
Control
E2
DPN
E2+PHTPP
F
Mean no of mitoses / HPF
p<0.001
p=0.001
Control
E2
E2+PHTPP
DPN
PHTPP
G
Luminal
No. of mamospheres /well
p=0.03
p=0.02
p=0.04
Control
E2
E2+ PHTPP
PHTPP
H
Triple-neg
No. of mamospheres /well
p<0.001
p=0.001
p<0.001
p<0.001
Control
DPN
PHTPP
DPN+PHTPP
I
HCI001
Tumor volume (mm3)
p=0.002
p<0.001
Control
DPN
PHTPP
DPN+PHTPP
J
HCI002
Tumor volume (mm3)
Control
DPN
PHTPP
DPN+PHTPP
K
HCI001
Control
DPN
PHTPP
DPN+PHTPP
Tumor volume (mm3)
Days
L
HCI002
Contol
DPN
PHTPP
DPN+PHTPP
Tumor volume (mm3)
Days

ARTICLE

MDA-MB-231 cells with Tet-on inducible ERβ shRNA into the intact NOD/SCID mice. Knockdown of ERβ reduced the tumor volume by more than 50.0% ($P = .01$) (confirmed in Supplementary Figure 5, E and F, available online) compared with the scrambled control (Figure 5C; Supplementary Figure 5D, available online). Furthermore, we injected wild-type MDA-MB-231 cells into the intact NOD/SCID mice. By treating with PHTPP during tumor growth, we observed a reduction of tumor volume at the five-week end point, although statistically nonsignificant (Figure 5D; Supplementary Figure 5G, available online).

As expected, in MCF7 mammosphere-derived xenografts, E2 treatment caused a nearly eight-time increase ($P = .001$) in the number of mitotic cells compared with the untreated control, whereas PHTPP almost completely neutralized ($P < .001$) this effect (Figure 5F). Nearly 50.0% of the tumor cells in the untreated control group were positive for ALDH1, reflecting the high expression of ALDH1 in mammospheres (Figure 5E, left panel). The level of $ALDH1^{High}$ cells was retained in the DPN- and E2-treated groups. Most interestingly, in tumors from the combined E2+PHTPP group, very few $ALDH1^{High}$ cells were observed (Figure 5E, right panel). This finding not only reflects a tumor-regressive effect by PHTPP but also indicates a potential to reduce BSCs numbers.

We then sought to further investigate the tumor-suppressive role of PHTPP by treating BSCs isolated from patients with luminal A (ER+/PR+/Her2-) and triple-negative (ER-/PR-/Her2-) breast carcinomas (Figure 5, G and H). As described earlier, E2 or DPN consistently induced mammosphere formation (41.4%, $P = .02$, and 22.6%, $P = .001$, respectively), whereas cotreatment with PHTPP completely abolished this stimulatory effect of E2 ($P = .03$) or DPN ($P < .001$). Moreover, PHTPP alone caused a statistically significant reduction of mammosphere numbers compared with the untreated control (53.7% reduction in Luminal tumors, $P = .04$, and 45.5% reduction in TNBC tumors, $P < .001$). This further indicates that ERβ is important for BSC maintenance and proliferation.

Targeted therapies for patients with triple-negative breast cancers (TNBCs) are lacking. Hence, to further investigate the possibility of targeting ERβ, two triple-negative patient-derived xenografts (PDXs) expressing endogenous ERβ (Supplementary Figure 5I, available online), HCI001 and HCI002, were established and assigned into different treatment groups. At end point, DPN treatment resulted in the largest tumor volumes in both models and PHTPP single treatment reduced tumor growth ($P < .001$ in HCI001) (Supplementary Figure 5H, available online). Moreover, when PHTPP was cosupplied, it could gradually neutralize the stimulatory effect of DPN on tumor growth ($P = .002$ in HCI001) (Figure 5, I–L). This further indicates that targeting ERβ is a possible therapeutic strategy in TNBCs.

Combining Tamoxifen With an ERβ Antagonist in a Xenograft Model

We sought to evaluate whether a combination of tamoxifen and ERβ modulator would be more efficient to block tumor growth as a consequence of ERβ expression in BSCs. Orthotopically injected MCF7 cells were allowed to form palpable tumors in NOD/SCID mice. As expected, tamoxifen caused a dramatic inhibition of tumor growth but was unable to completely eliminate the tumor (Figure 6A; Supplementary Figure 6, available online). Combining tamoxifen with PHTPP caused a gradual decrease of tumor size with increasing concentration of PHTPP (Figure 6B), further indicating that PHTPP improves the response to tamoxifen.

Discussion

The current dogma of BSCs as more or less estrogen insensitive does not fully reflect the central importance of estrogens as key factors for tumor growth. Although ERα is exclusively expressed in the luminal breast cancer subtypes (30), the expression of ERα is completely negative in BSCs. In contrast, we found that ERβ was expressed at similar levels within all breast cancer subtypes. ERβ protein was identified in the majority of BSCs, but its expression declined as the BSCs differentiated. We also observed an increase of ERβ mRNA upon mammosphere formation. Our findings are in line with an earlier study reporting elevated ERβ expression in basal/stem cell populations (31).

We investigated the molecular function of ERβ in BSCs and observed a strong increase in sphere formation upon treatment with E2 or DPN. This effect was observed in repeated assays from patients with varying primary tumor characteristics. As a consequence of ERα absence, treatment with its agonist PPT did not affect the number of mammospheres, nor did tamoxifen or fulvestrant. We have recently shown that tamoxifen activates

ARTICLE

Figure 5. Tumor growth and mammosphere formation in response to estrogen receptor (ER)β inhibition. Ovariectomized NOD/SCID mice were implanted with either **(A)** $1x10^6$ adherent MCF7 cells (n = 5 mice/group, tumor take rate = 77.5%) or **(B)** $5x10^5$ MCF7-derived mammospheres (n = 4 mice/group, tumor take rate = 85.0%) into the fourth mammary gland fat pads and randomly assigned to control or treatment groups (control DMSO: diarylproprionitrile [DPN; 4 mg/kg]; PPT [10 mg/kg]; E2 [0.1 mg/kg]; PHTPP [4 mg/kg]). Treatments were given by daily injections. The final tumor volume (mm^3) was determined (Student's *t* test, mean ± SD). **C)** Intact NOD/SCID mice were transplanted with 2 $x10^6$ doxycycline inducible shRNA-ERβ MDA231 cell or scrambled control shRNA transcended MDA-MB-231 cells (Student's *t* test, mean± SD, n = 4 mice/group, tumor take rate = 100.0%). Doxycycline (2 mg/mL) was provided in the drinking water. **D)** Intact NOD/SCID mice were transplanted with 2 $x10^6$ MDA231 cells for control (vehicle) and PHTPP treatment groups (n = 4 mice/group, tumor take rate = 100.0%). The treatments were given by injections every second day. Tumors were resected at end point and tumor volume was calculated (Student's *t* test, mean ± SD). **E)** Immunohistochemical staining of ALDH1 in MCF7 xenografts from Figure 5B. Because of the very small size of PHTPP-treated tumors, ALDH1-staining could not be performed. The **left panel** represents average values (0, 0.0%; 1, 1.0%–10.0%; 2, 10.0%–50.0%; 3, 50.0%–100.0%, positive cytoplasmic stained cells) (Student's *t* test, mean± SD, n = 3 counts). **Right panel**: representative images for ALDH1-staining. **Scale bar** = 10 μm. **F)** Average number of mitoses/high-power field (40x) ± SD. Experiments were performed in three tumors per group (Student's *t* test, mean ± SD). Mammosphere formation from **(G)** luminal A (n = 4 patients, 4 replicates) or **(H)** triple-negative (n = 3 patients, 4 replicates) patient-derived cancer cells. Five hundred to 1000 cells from dissociated primary breast cancer mammospheres were plated onto 48-well plates incubated with 10 nM E2, 100 nM PHTPP, 10 nM DPN, 10 nM E2 + 100 nM PHTPP combination, or vehicle control for 12 days (Student's *t* test, mean ± SD). Four-week-old NOD/SCID mice were transplanted with 2 mm^3 tumor pieces from PDX HCI001 (n = 5 mice/group, tumor take rate = 100%) **(I)** or HCI002 (n = 5 mice/group, tumor take rate = 90%) **(J)** and supplemented with DPN (4 mg/kg), PHTPP (4 mg/kg), or combination treatment every other day. Treatments started when tumor initiation reached at least 3 mm^3, and tumor volume was measured at the same time of injection. **I and J)** Tumor volume (mm^3) after end point was calculated (Student's *t* test, mean ± SD). **K and L)** Effect of ERβ agonist and antagonist on triple-negative patient-derived xenografts. **Lines** show mean of tumor volumes from each treatment group; **error bars** represent SD. All statistical tests were two-sided. DPN = diarylproprionitrile; HCI001/002 = patient-derived xenograft models; PPT = propylpyrazoletrisphenol.

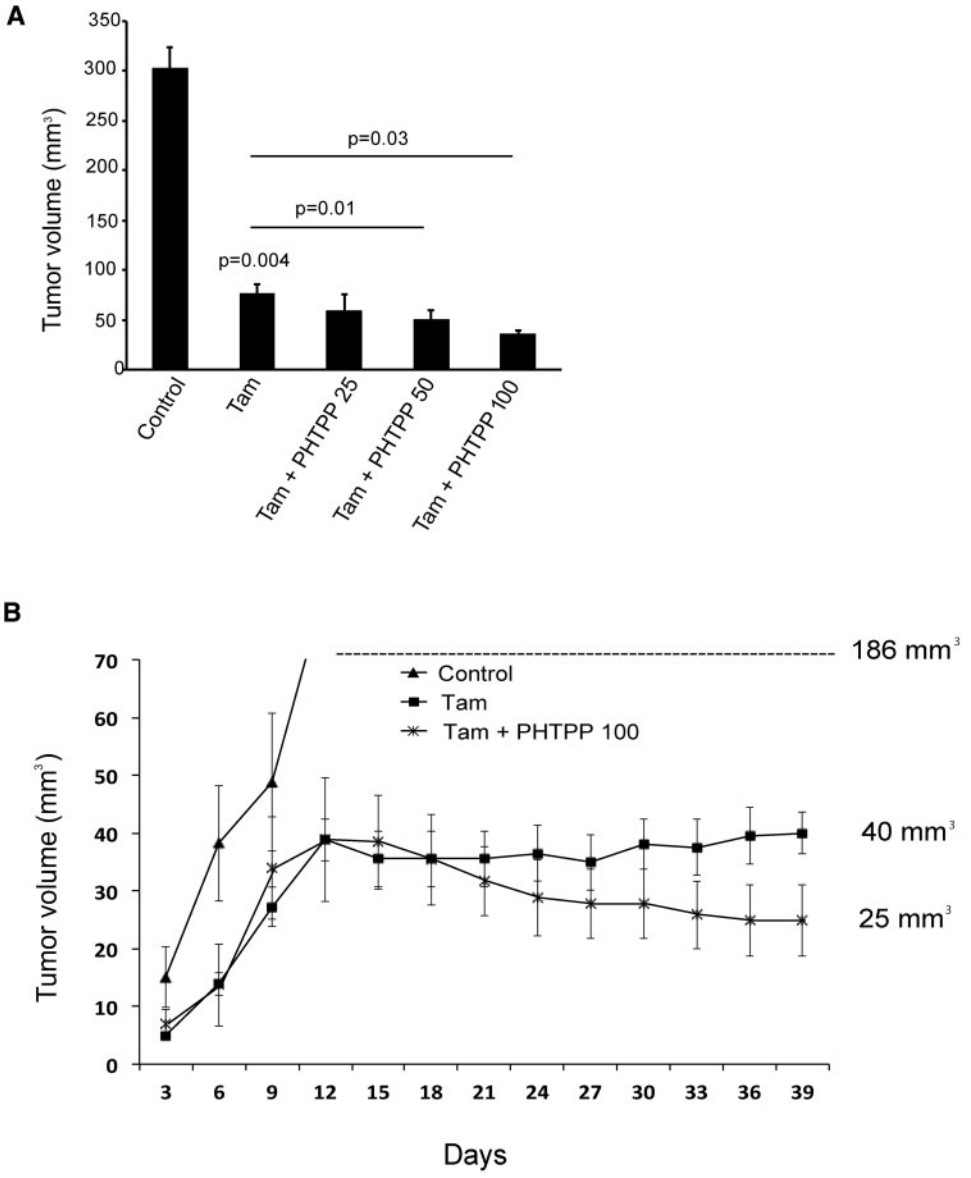

Figure 6. Effects on tumor growth by a combination of tamoxifen and an estrogen receptor (ER)β antagonist. Eight-week-old NOD/SCID mice were injected with $1x10^6$ MCF7 cells and supplemented with tamoxifen citrate (1 mg/kg), or combined with different concentrations of PHTPP by injections (n = 4 mice/group, tumor take rate = 75%). Treatment started on day 14, and MCF7 tumor volume was measured every third day. **A)** Tumor volume (mm^3) was determined after mice were killed at day 39 (Student's *t* test, mean ± SD). **B)** The **number after each curve** indicates the final measurement of in vivo tumor volume. **Lines** show mean of tumor volumes from each treatment group; **error bars** represent SD. All statistical tests were two-sided. Tam = tamoxifen (1 mg/kg); Tam + PHTPP 25 = tamoxifen (1 mg/kg) + PHTPP (1 mg/kg); Tam + PHTPP 50 = tamoxifen (1 mg/kg) + PHTPP (2 mg/kg); Tam + PHTPP 100 = tamoxifen (1 mg/kg) + PHTPP (4 mg/kg).

mTOR-regulated ribosomal synthesis and is insufficient to inhibit proliferation in BSCs (32). Our findings shed light on the incapability of current endocrine agents to completely eradicate all tumor cells as a proportion of breast cancers relapse after or during adjuvant endocrine therapy.

Breast cancer cell lines exhibit very low levels of ERβ mRNA and are considered ERβ-negative by many research groups; therefore, ERβ function has primarily been studied by exogenous transfer of ERβ expression vectors. ERβ is generally considered an antiproliferative mediator with proposed tumor-suppressive activity in ERα-positive cell lines (33), but proliferative effects have been noted in some circumstances and a bifaceted role of ERβ has been suggested (34,35). Importantly, we only observed a proliferative function of ERβ in the nonadherent malignant mammosphere state and in vivo, not in the adherent state in vitro. Most probably this is a consequence of the low ERβ levels in adherent cancer cells. In addition, the sphere-forming capacity was further enhanced by ERβ overexpression. Hence, our study also demonstrates the suboptimal capability of adherently growing cell lines to reflect all aspects of tumor biology.

Patient-derived mammospheres are hard to isolate and expand, complicating mechanistic studies. We and others have found that mammospheres generated from MCF7 are to an extent a sufficient complement for mechanistic studies (22). We observed a marked increase in ERβ expression when adherent cells formed mammospheres, correlating with a shift from a high to low ERα/ERβ ratio. It has recently been shown that CSCs

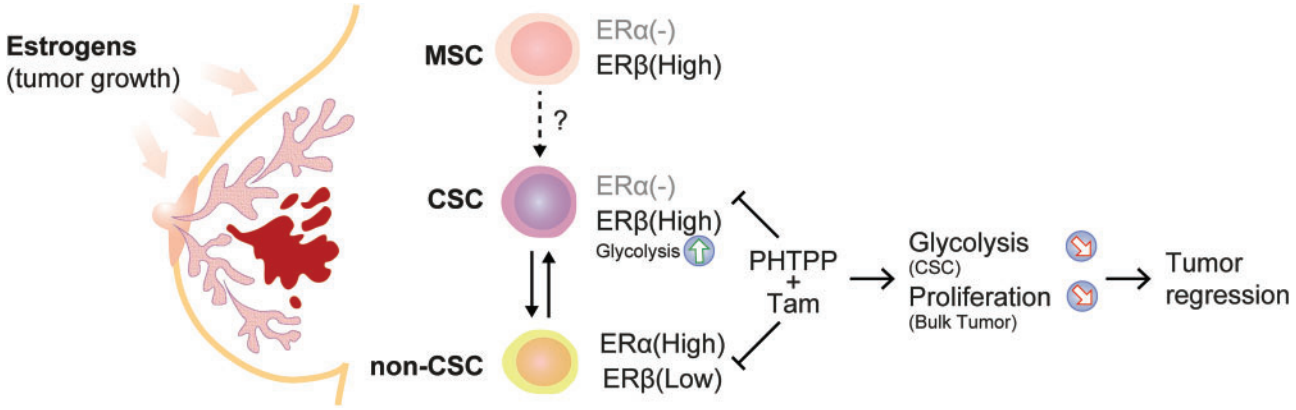

Figure 7. Hypothetical overview of estrogen receptor (ER)β function during breast carcinogenesis. We propose a dual function of ERβ in the human mammary gland depending on a "neoplastic switch," from a potential inhibitor of mammary stem cell proliferation to an activator in the malignant counterpart. 1) Stimulation of ERβ in normal mammary stem cells decreases proliferation. 2) ERβ drives proliferation in breast cancer cells with tumor-initiating capabilities in the presence of ERβ agonist by inducing glycolytic metabolism, which is essential for CSCs maintenance. 3) In the differentiated primary tumor that is mainly ERα-positive, estrogen induces proliferation as described elsewhere. 4) We propose that by combining standard endocrine therapy (tamoxifen) with an ERβ-selective antagonist (PHTPP) a more profound tumor regression can be achieved through targeting cancer cells with both differentiated and stem-cell phenotypes. CSC = cancer stem cells; ER = estrogen receptor; MSC = mammary stem cells.

isolated from several solid tumors display altered energy metabolism and are more glycolytic compared with differentiated tumor cells (27,36–38). Furthermore, upregulation of glycolysis correlates with increased tumor aggressiveness and multidrug resistance (40,41). Using whole-transcriptome analysis of MCF7-derived mammospheres, we observed the induced glycolysis process upon stimulation of ERβ. This correlated with increased L-lactate concentrations in the growth media from both patient-derived and MCF7 mammospheres, indicating increased anaerobic glycolysis. Ciavardelli et al. reported that BSCs are less dependent on the mitochondrial activity than normal cancer cells and primarily rely on glycolysis for ATP production (26). Accumulating evidence also suggests that mitochondria are important targets for the actions of estrogens (42,43), based on the observation that ERβ localizes in mitochondria in various cells (42,44–49). ERβ knockdown leads to a mild mitochondrial uncoupling phenotype (50), while activation of ERβ negatively affects oxidative phosphorylation and compromises mitochondrial complexes activity (51). In adherent breast cancer cells, the introduction of overexpressed ERβ causes a strong inhibition of cell proliferation due to the increase of apoptosis through the mitochondrial pathway (52–54). Unlike differentiated cancer cells, CSCs are not entirely dependent on mitochondrial oxidative respiration; therefore, ERβ as a vulnerability factor for mitochondria might be beneficial for CSC maintenance by enhancing glycolytic shift metabolism. Consistent with these studies, our OCR analyses of MCF7S revealed that DPN stimulation reduced the oxygen consumption rate and could be rescued by the ERβ antagonist PHTPP. Furthermore, MCF7S with knockdown of ERβ expressed lower levels of glycolytic genes and higher levels of mitochondrial genes compared with the control. Consequently, ERβ-mediated impaired mitochondrial function could further aid in the switch toward glycolytic metabolism for ATP production, BSC maintenance, and proliferation.

Based on our xenograft data, we demonstrate that endogenous ERβ is proliferative in luminal and triple-negative breast cancer mouse models and can be targeted by PHTPP. We suggest that an ERβ antagonist combined with tamoxifen or, alternatively, combined with an aromatase inhibitor should be studied as adjuvant therapy for luminal breast cancer patients, thereby targeting both the more differentiated (mainly ERα[+]) cells as well as the stem-like, poorly differentiated cells (ERα[-]/ERβ[+])(Figure 7). But we also suggest that ERβ-selective antagonists should be further investigated for patients with ERα-negative tumors, clinically considered hormone independent and not candidates for regular endocrine therapy.

However, there are limitations of our study. First, because of the low expression level of endogenous ERβ in cell line–derived spheres, we could not observe massive changes at mRNA level when exploring the function of ERβ in BSCs, despite ERβ knockdown or stimulation by DPN. There are also important biological restrictions of using cell lines as cancer models, and sophisticated experimental methods should be optimized for the small amount of patient-derived material to further support our data. In addition, we observed that PHTPP is not a complete ERβ antagonist and more selective ERβ-antagonists should be developed for clinical trials.

Our study highlights the importance of ERβ in breast cancer. In contrast to the idea of stem cells as responders to estrogens through paracrine signaling, we propose the novel concept of BSCs as directly estrogen sensitive through ERβ, in turn shedding light on the mechanism of estrogen action during breast carcinogenesis. We hope that the identification of stem cell–enriched ERβ and its putative ERβ antagonist could be utilized as a stem cell–specific therapy to hit breast cancer fully.

Funding

This work was supported with grants from Swedish Society of Medicine, Swedish Society for Medical Research (SSMF), and Magnus Bergvalls Stiftelse (to JH); the Karolinska Institute's Theme Center in Breast Cancer (BRECT) support and the Linnécenter for Prevention of Breast and Prostate cancer (CRisP; to GR); Swedish Cancer Society, Stockholm Cancer Society, King Gustav V Jubilee Fund, Karolinska Institutet, and Stockholm County Council Research Strategy Committee, Swedish Breast Cancer Association (to JH); and

ARTICLE

the Science for Life–Astra Zeneca collaborative grant, Marie Curie Actions FP7-PEOPLE-2011-COFUND (GROWTH 291795) via the VINNOVA program Mobility for Growth (to CW).

Notes

The study sponsors had no role in the study design; the collection or interpretation of the data; the writing of the manuscript; or the decision of submission.

The authors have no potential conflicts of interest to declare.

We thank Melissa Landis of the Houston Methodist Hospital Research Institute TX and Jonas Bergh of the Karolinska Institutet for advice and critical comments to the manuscript; Uta Rabenhorst, Camilla Cristando, and Agneta Birgitta Andersson for the technical support; and the Huntsman Cancer Institute in Salt Lake City, Utah, for the use of the Preclinical Research Resource (PRR), which provided PDX model service. We thank Lennart Blomqvist for collecting the benign breast reduction material. We also thank the Stockholm Medical Biobank for structural and economical support and Stefan Nilsson and KaroBio AB for valuable comments and help in the study.

References

1. Dontu G, Abdallah WM, Foley JM, et al. In vitro propagation and transcriptional profiling of human mammary stem/progenitor cells. *Genes Dev*. 2003; 17(10):1253–1270.
2. Reynolds BA, Tetzlaff W, Weiss S. A multipotent EGF-responsive striatal embryonic progenitor cell produces neurons and astrocytes. *J Neurosci*. 1992; 12(11):4565–4574.
3. Al-Hajj M, Wicha MS, Benito-Hernandez A, et al. Prospective identification of tumorigenic breast cancer cells. *Proc Natl Acad Sci U S A*. 2003;100(7): 3983–3988.
4. Ma R, Fredriksson I, Karthik GM, et al. Superficial scrapings from breast tumors is a source for biobanking and research purposes. *Lab Invest*. 2014;94(7): 796–805.
5. Ginestier C, Hur MH, Charafe-Jauffret E, et al. ALDH1 is a marker of normal and malignant human mammary stem cells and a predictor of poor clinical outcome. *Cell Stem Cell*. 2007;1(5):555–567.
6. Morimoto K, Kim SJ, Tanei T, et al. Stem cell marker aldehyde dehydrogenase 1-positive breast cancers are characterized by negative estrogen receptor, positive human epidermal growth factor receptor type 2, and high Ki67 expression. *Cancer Sci*. 2009;100(6):1062–1068.
7. Davies C, Godwin J, Gray R, et al. Relevance of breast cancer hormone receptors and other factors to the efficacy of adjuvant tamoxifen: Patient-level meta-analysis of randomised trials. *Lancet*. 2011;378(9793):771–784.
8. Honma N, Horii R, Iwase T, et al. Clinical importance of estrogen receptor-beta evaluation in breast cancer patients treated with adjuvant tamoxifen therapy. *J Clin Oncol*. 2008;26(22):3727–3734.
9. Gruvberger-Saal SK, Bendahl PO, Saal LH, et al. Estrogen receptor beta expression is associated with tamoxifen response in ERalpha-negative breast carcinoma. *Clin Cancer Res*. 2007;13(7):1987–1994.
10. Rosin G, de Boniface J, Karthik GM, et al. Oestrogen receptors beta1 and betacx have divergent roles in breast cancer survival and lymph node metastasis. *Br J Cancer*. 2014;111(5):918–926.
11. Paech K, Webb P, Kuiper GG, et al. Differential ligand activation of estrogen receptors ERalpha and ERbeta at AP1 sites. *Science*. 1997;277(5331):1508–1510.
12. Asselin-Labat ML, Vaillant F, Sheridan JM, et al. Control of mammary stem cell function by steroid hormone signalling. *Nature*. 2010;465(7299):798–802.
13. Russo J, Snider K, Pereira JS, et al. Estrogen induced breast cancer is the result in the disruption of the asymmetric cell division of the stem cell. *Horm Mol Biol Clin Investig*. 2010;1(2):53–65.
14. Mallepell S, Krust A, Chambon P, et al. Paracrine signaling through the epithelial estrogen receptor alpha is required for proliferation and morphogenesis in the mammary gland. *Proc Natl Acad Sci U S A*. 2006;103(7):2196–2201.
15. Fillmore CM, Gupta PB, Rudnick JA, et al. Estrogen expands breast cancer stem-like cells through paracrine FGF/Tbx3 signaling. *Proc Natl Acad Sci U S A*. 2010;107(50):21737–21742.
16. Miller LD, Smeds J, George J, et al. An expression signature for p53 status in human breast cancer predicts mutation status, transcriptional effects, and patient survival. *Proc Natl Acad Sci U S A*. 2005;102(38):13550–13555.
17. Liu Y, Nenutil R, Appleyard MV, et al. Lack of correlation of stem cell markers in breast cancer stem cells. *Br J Cancer*. 2014;110(8):2063–2071.
18. Pece S, Tosoni D, Confalonieri S, et al. Biological and molecular heterogeneity of breast cancers correlates with their cancer stem cell content. *Cell*. 2010; 140(1):62–73.
19. Hutson SW, Cowen PN, Bird CC. Morphometric studies of age related changes in normal human breast and their significance for evolution of mammary cancer. *J Clin Pathol*. 1985;38(3):281–287.
20. Klevebring D, Rosin G, Ma R, et al. Sequencing of breast cancer stem cell populations indicates a dynamic conversion between differentiation states in vivo. *Breast Cancer Res*. 2014;16(4):R72.
21. Gupta PB, Fillmore CM, Jiang G, et al. Stochastic state transitions give rise to phenotypic equilibrium in populations of cancer cells. *Cell*. 2011;146(4):633–644.
22. Fillmore CM, Kuperwasser C. Human breast cancer cell lines contain stem-like cells that self-renew, give rise to phenotypically diverse progeny and survive chemotherapy. *Breast Cancer Res*. 2008;10(2):R25.
23. Masiakowski P, Breathnach R, Bloch J, et al. Cloning of cDNA sequences of hormone-regulated genes from the MCF-7 human breast cancer cell line. *Nucleic Acids Res*. 1982;10(24):7895–7903.
24. Clark GM, McGuire WL. Progesterone receptors and human breast cancer. *Breast Cancer Res Treat*. 1983;3(2):157–163.
25. Compton DR, Sheng S, Carlson KE, et al. Pyrazolo[1,5-a]pyrimidines: Estrogen receptor ligands possessing estrogen receptor beta antagonist activity. *J Med Chem*. 2004;47(24):5872–5893.
26. Ciavardelli D, Rossi C, Barcaroli D, et al. Breast cancer stem cells rely on fermentative glycolysis and are sensitive to 2-deoxyglucose treatment. *Cell Death Dis*. 2014;5:e1336.
27. Palorini R, Votta G, Balestrieri C, et al. Energy metabolism characterization of a novel cancer stem cell-like line 3AB-OS. *J Cell Biochem*. 2014;115(2):368–379.
28. Gutierrez MC, Detre S, Johnston S, et al. Molecular changes in tamoxifen-resistant breast cancer: Relationship between estrogen receptor, HER-2, and p38 mitogen-activated protein kinase. *J Clin Oncol*. 2005;23(11):2469–2476.
29. Li X, Lewis MT, Huang J, et al. Intrinsic resistance of tumorigenic breast cancer cells to chemotherapy. *J Natl Cancer Inst*. 2008;100(9):672–679.
30. Sorlie T, Perou CM, Tibshirani R, et al. Gene expression patterns of breast carcinomas distinguish tumor subclasses with clinical implications. *Proc Natl Acad Sci U S A*. 2001;98(19):10869–10874.
31. Lawson DA, Bhakta NR, Kessenbrock K, et al. Single-cell analysis reveals a stem-cell program in human metastatic breast cancer cells. *Nature*. 2015; 526(7571):131–135.
32. Karthik GM, Ma R, Lovrot J, et al. mTOR inhibitors counteract tamoxifen-induced activation of breast cancer stem cells. *Cancer Lett*. 2015;367(1):76–87.
33. Strom A, Hartman J, Foster JS, et al. Estrogen receptor beta inhibits 17beta-estradiol-stimulated proliferation of the breast cancer cell line T47D. *Proc Natl Acad Sci U S A*. 2004;101(6):1566–1571.
34. Leygue E, Murphy LC. A bi-faceted role of estrogen receptor beta in breast cancer. *Endocr Relat Cancer*. 2013;20(3):R127–R139.
35. Jonsson P, Katchy A, Williams C. Support of a bi-faceted role of estrogen receptor beta (ERbeta) in ERalpha-positive breast cancer cells. *Endocr Relat Cancer*. 2014;21(2):143–160.
36. Gammon L, Biddle A, Heywood HK, et al. Sub-sets of cancer stem cells differ intrinsically in their patterns of oxygen metabolism. *PLoS One*. 2013;8(4):e62493.
37. Yuan S, Wang F, Chen G, et al. Effective elimination of cancer stem cells by a novel drug combination strategy. *Stem Cells*. 2013;31(1):23–34.
38. Zhou Y, Zhou Y, Shingu T, et al. Metabolic alterations in highly tumorigenic glioblastoma cells: Preference for hypoxia and high dependency on glycolysis. *J Biol Chem*. 2011;286(37):32843–32853.
39. Morfouace M, Lalier L, Bahut M, et al. Comparison of spheroids formed by rat glioma stem cells and neural stem cells reveals differences in glucose metabolism and promising therapeutic applications. *J Biol Chem*. 2012;287(40): 33664–33674.
40. Milane L, Duan Z, Amiji M. Role of hypoxia and glycolysis in the development of multi-drug resistance in human tumor cells and the establishment of an orthotopic multi-drug resistant tumor model in nude mice using hypoxic pre-conditioning. *Cancer Cell Int*. 2011;11:3.
41. Harris AL. Hypoxia—a key regulatory factor in tumour growth. *Nat Rev Cancer*. 2002;2(1):38–47.
42. Chen JQ, Yager JD, Russo J. Regulation of mitochondrial respiratory chain structure and function by estrogens/estrogen receptors and potential physiological/pathophysiological implications. *Biochim Biophys Acta*. 2005;1746(1):1–17.
43. Felty Q, Roy D. Estrogen, mitochondria, and growth of cancer and non-cancer cells. *J Carcinog*. 2005;4(1):1.
44. Chen JQ, Delannoy M, Cooke C, et al. Mitochondrial localization of ERalpha and ERbeta in human MCF7 cells. *Am J Physiol Endocrinol Metab*. 2004;286(6): E1011–E1022.
45. Herrick SP, Waters EM, Drake CT, et al. Extranuclear estrogen receptor beta immunoreactivity is on doublecortin-containing cells in the adult and neonatal rat dentate gyrus. *Brain Res*. 2006;1121(1):46–58.
46. Mehra RD, Sharma K, Nyakas C, et al. Estrogen receptor alpha and beta immunoreactive neurons in normal adult and aged female rat hippocampus: A qualitative and quantitative study. *Brain Res*. 2005;1056(1):22–35.
47. Milner TA, Ayoola K, Drake CT, et al. Ultrastructural localization of estrogen receptor beta immunoreactivity in the rat hippocampal formation. *J Comp Neurol*. 2005;491(2):81–95.

48. Solakidi S, Psarra AM, Sekeris CE. Differential subcellular distribution of estrogen receptor isoforms: Localization of ERalpha in the nucleoli and ERbeta in the mitochondria of human osteosarcoma SaOS-2 and hepatocarcinoma HepG2 cell lines. *Biochim Biophys Acta*. 2005;1745(3):382–392.
49. Yang SH, Liu R, Perez EJ, et al. Mitochondrial localization of estrogen receptor beta. *Proc Natl Acad Sci U S A*. 2004;101(12):4130–4135.
50. Yang SH, Sarkar SN, Liu R, et al. Estrogen receptor beta as a mitochondrial vulnerability factor. *J Biol Chem*. 2009;284(14):9540–9548.
51. Manente AG, Valenti D, Pinton G, et al. Estrogen receptor beta activation impairs mitochondrial oxidative metabolism and affects malignant mesothelioma cell growth in vitro and in vivo. *Oncogenesis*. 2013;2:e72.
52. Lazennec G, Bresson D, Lucas A, et al. ER beta inhibits proliferation and invasion of breast cancer cells. *Endocrinology*. 2001;142(9):4120–4130.
53. Cheng J, Lee EJ, Madison LD, et al. Expression of estrogen receptor beta in prostate carcinoma cells inhibits invasion and proliferation and triggers apoptosis. *FEBS Lett*. 2004;566(1-3):169–172.
54. Treeck O, Pfeiler G, Horn F, et al. Novel estrogen receptor beta transcript variants identified in human breast cancer cells affect cell growth and apoptosis of COS-1 cells. *Mol Cell Endocrinol*. 2007;264(1–2):50–60.